



Describing fatigue crack growth and load ratio effects in Al 2524 T3 alloy with an enhanced exponential model

C.A.R.P. Baptista^{a,*}, A.M.L. Adib^b, M.A.S. Torres^c, V.A. Pastoukhov^d

^a Escola de Engenharia de Lorena, EEL-USP, Department of Materials Engineering, Cx. Postal 116, CEP 12602-810 Lorena/SP, Brazil

^b Empresa Brasileira de Aeronáutica S.A., EMBRAER, CEP 12227-901 São José dos Campos/SP, Brazil

^c Faculdade de Engenharia de Guaratinguetá, FEG-UNESP, Department of Mechanics, CEP 12516-410, Guaratinguetá/SP, Brazil

^d Universidade de Taubaté, UNITAU, Institute of Engineering, CEP 12080-000 Taubaté/SP, Brazil

ARTICLE INFO

Article history:

Received 21 March 2011

Received in revised form 3 April 2012

Available online 13 April 2012

Keywords:

Fatigue crack growth

Exponential model

Cycle asymmetry

Aluminum alloy 2524

ABSTRACT

The fatigue crack behavior in metals and alloys under constant amplitude test conditions is usually described by relationships between the crack growth rate da/dN and the stress intensity factor range ΔK . In the present work, an enhanced two-parameter exponential equation of fatigue crack growth was introduced in order to describe sub-critical crack propagation behavior of Al 2524-T3 alloy, commonly used in aircraft engineering applications. It was demonstrated that besides adequately correlating the load ratio effects, the exponential model also accounts for the slight deviations from linearity shown by the experimental curves. A comparison with Elber, Kujawski and “Unified Approach” models allowed for verifying the better performance, when confronted to the other tested models, presented by the exponential model.

© 2012 Elsevier Ltd. All rights reserved.

1. Introduction

Fatigue crack growth (FCG) is a main issue in the life prediction and maintenance of aircraft structures (Molent and Barter, 2007). The FCG behavior in metals and alloys under constant amplitude test conditions is usually described by the relationship between the crack growth rate da/dN and the stress intensity factor range ΔK . The typical log–log plots of da/dN versus ΔK shown schematically in Fig. 1 have a sigmoidal shape that can be divided into three regions (Stephens et al., 2001; Suresh, 1998; Jones et al., 2008; Kohout, 1999). Region I is the near-threshold region, in which the curve becomes steep and appears to approach an asymptote ΔK_{th} , a lower limiting ΔK value below which no crack growth is expected to occur. Region II (intermediate regime) corresponds to stable macroscopic crack growth. Region III is associated with rapid crack growth just prior to final failure and is controlled primarily by K_{IC} ,

the fracture toughness for the material and thickness of interest. A significant portion of fatigue life of mechanical components is occupied in the subcritical crack growth (Region II) (Stephens et al., 2001; Dowling, 1999). In several parts, particularly those made from sheets or plates and containing stress concentrators (such as rivet holes), the existence of a crack is assumed *a priori* and determining the number of cycles it takes to reach the critical size (Region III) is a design criterion, from which the non-destructive inspection intervals is established (Dowling, 1999; Lee et al., 2005).

For Region II, where the medium crack propagation rates (10^{-8} – 10^{-6} m/cycle) occur, an empirical relationship proposed by Paris and Erdogan (1963) was written in the form of Eq. (1), which means a straight line in the log–log fit and where the scaling constants C and n should represent the FCG resistance of a given material. The Paris potential equation, in which ΔK is the main driving force for fatigue crack growth, became the canonic FCG model:

$$\frac{da}{dN} = C \Delta K^n \quad (1)$$

* Corresponding author. Tel.: +55 12 3159 9914; fax: +55 12 3153 3006.
E-mail address: baptista@demar.eel.usp.br (C.A.R.P. Baptista).

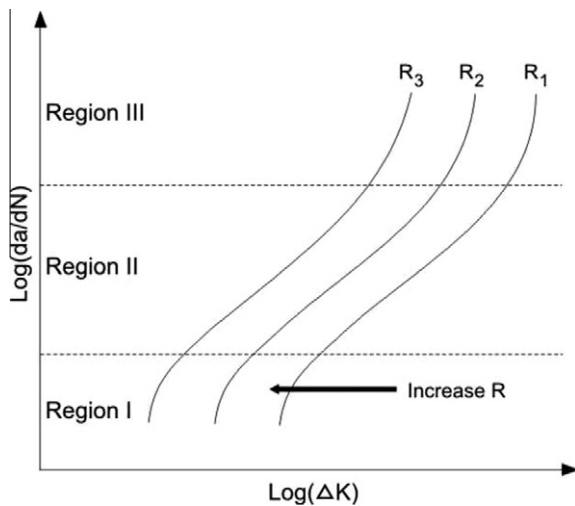


Fig. 1. Total FCG curves for various load ratios.

It is long observed that, for a fixed ΔK , da/dN is strongly influenced by the stress-cycle asymmetry, usually expressed in terms of the load ratio R (K_{min}/K_{max}) (Broek and Shijve, 1963; Forman et al., 1967; Walker, 1970). The threshold stress intensity values (ΔK_{th}) were found to depend on R as well (Stephens et al., 2001; Vasudevan and Sadananda, 1996). Fig. 1 also shows the crack growth rate curves under different R -ratios, indicating that increasing R has a tendency to increase da/dN in all portions of the sigmoidal curve (Stephens et al., 2001). From this finding, diverse attempts were done in order to obtain the collapse of several curves produced from da/dN and ΔK with different R to a single curve (Elber, 1971; Noroozi et al., 2007; Xiaoping and Torgeir, 2007; Kujawski, 2001).

An important result for the proposed question was given by Elber (1971) that introduced the concepts of crack closure (K_{cl}) and effective cyclic stress intensity factor (ΔK_{eff}) to explain the effects of R -ratio on fatigue crack growth in the form of Eq. (2):

$$\frac{da}{dN} = C(\Delta K_{eff})^n, \quad \Delta K_{eff} = (K_{max} - K_{cl}) \quad (2)$$

where K_{cl} is the stress intensity factor corresponding to the stress for which the crack remains closed.

Elber assumed that the crack faces remain in contact during part of the loading cycle. Then ΔK_{eff} , which depends on R , corresponds to a fraction of ΔK in which the crack remains open. Thus, Eq. (2) leads to results for the constants C and n independent of load ratio R . The closure concept gives a physical explanation for the so-called R -effects, but discussions persist about the efficacy of this approach. Louat et al. (1993) presented the conceptual and experimental difficulties that emerge when the crack closure is evaluated. Comparative analyses indicated that the opening load value (necessary to calculate K_{cl}) depends on the position and the measurement technique. Therefore, the description of FCG behavior in terms of ΔK_{eff} is impaired by the various experimental and conceptual difficulties associated with the estimation of crack closure. These include the verification of contradictory results of closure

loading measurements (Philips, 1989; Newman and Elber, 1988), the observation of influences of the location and employed technique on the crack opening load value (Macha et al., 1979; Shin and Smith, 1985) and the identification of the different closure mechanisms and their relative importance in each specific situation (Louat et al., 1993; Skelton and Haigh, 1978; Ritchie and Suresh, 1982; McClung, 1991). Despite this criticism, the crack closure phenomenon has been largely accepted to explain many aspects of crack behavior in metallic materials, including R -effects, variable amplitude loading, microstructure, environment and the magnitude of fatigue threshold (Alizadeh et al., 2007; Ismonov and Daniewicz, 2010).

However, it is a fact that the substitution of ΔK by ΔK_{eff} in Eq. (1) maintains the imposition of the stress intensity range as the only driving force for FCG. On the other hand, is known that the unambiguous definition of a cyclic loading needs the use of two independent parameters. From the five parameters usually employed to define cyclic loaded cracks (K_{max} , K_{min} , K_{mean} , ΔK , R), only any two of them are independent (Sadananda and Vasudevan, 2004). In general, the variation of any of the loading parameters (except for ΔK), can cause significant changes in the values of the C , n constants of Eq. (1). Thus, a way to collapse curves of different R without the need of the closure data is to consider da/dN as a function of two independent loading parameters (Zhang et al., 2005; McEvily and Ritchie, 1998). Walker's approach (Walker, 1970), in which the crack growth rate is given in terms of Eq. (3), was one of the first models to adopt two loading parameters. Eq. (3) is the same as Paris equation when R is zero. This model is capable of acting with $R > 0$ but has limitations for $R < 0$ (Xiaoping and Torgeir, 2007). Besides, Walker's approach does not consider as independent the effects of the loading parameters on the crack growth rate:

$$\frac{da}{dN} = C \Delta K^n (1 - R)^{n(m-1)} \quad (3)$$

More recently, Kujawski (2001) proposed a new mechanical driving force parameter for correlation of R -ratio effects on FCG without utilization of closure data. According to this proposal, the driving force is based on the positive part of the applied stress intensity factor range, ΔK^+ , and the maximum value assumed by the stress intensity factor in the load cycle, K_{max} . By adopting this new parameter, a FCG model was then developed by Kujawski and Dinda (2004) as Eq. (4):

$$\frac{da}{dN} = C(\Delta K^+)^n, \quad \Delta K^+ = (K_{max})^\alpha (\Delta K)^{1-\alpha} \quad (4)$$

In this model, the value of constant α is determined from the slopes of the straight lines fitted to the ΔK and K_{max} pairs at a given growth rate (Kujawski and Dinda, 2004). Kujawski states that by employing the ΔK^+ parameter a significant improvement was obtained in correlation of FCG data in comparison with the conventional Elber's closure approach.

Another way to describe the R -effects is to employ at least two of the loading parameters (K_{max} , K_{min} , K_{mean} , ΔK , R) which, acting independently, are capable of modeling each one of the original curves without collapsing them

as the previously described models did. The original idea of two driving forces for FCG was first introduced by Sadananda and Vasudevan and was called the Unified Approach (UA). These authors claim that fatigue crack growth rate should be represented in terms of two parameters ΔK and K_{max} since these are the two driving forces necessary for a crack to grow (Sadananda and Vasudevan, 1994, 2004, 2003a,b).

Maymon (2005) and Baptista et al. (2006) independently presented a potential bi-parametric model expressed by Eq. (5), in which f and g are two distinct loading parameters characterizing the driving forces at the crack tip, for example, ΔK and K_{max} . This natural improvement of the Walker model, based on UA, assumes as independent the exponents of the loading parameters. The model constants C , α , β are determined for a wide range of loading conditions. It is important to emphasize that this model is capable of predicting the FCG behavior under experimental conditions different from those employed in the calculation of its constants. Another characteristic of such a potential model is that, for the constants relationships given in Eq. (6), the same results are obtained for any two parameters that can be employed to define the loading cycle (Baptista et al., 2006):

$$\frac{da}{dN} = C(f)^\alpha (g)^\beta \quad (5)$$

$$C \Delta K^\alpha K_{max}^\beta = C \Delta K^{\alpha+\beta} (1-R)^{-\beta} = C K_{max}^{\alpha+\beta} (1-R)^\alpha \quad (6)$$

On the other hand, it is well known that the real fatigue data at each stress ratio can show a certain degree of non-linearity, given by changes in the slope of the da/dN - ΔK plots (Swain et al., 1990; Ishii et al., 1999). Recently a new exponential model, proposed by Adib and Baptista, has enabled the consideration of the non-linear Region II da/dN - ΔK behavior. For a single FCG curve, this Arrhenius-type relation, named $\alpha\beta$ model, is written in the form of Eq. (7) (Adib and Baptista, 2007):

$$\frac{da}{dN} = A \exp\left(\frac{\beta}{\Delta K}\right) \quad (7)$$

where $A = e^\alpha$, α and β being the fitting coefficients.

The FCG behavior of commercially pure titanium for a range of R -ratios was modeled using Eq. (7) by taking an average α_{av} and recalculated individual β_i values (Adib and Baptista, 2007). It was then verified that the R -effect is represented by the variation of these β_i values, and a linear relationship was obtained by plotting β_i against $\log R$.

The previous observations form the basis for an enhanced exponential equation of FCG, which is introduced in the present work. Furthermore, a comparison between FCG models including this new exponential equation, the two-parameter potential model, Eq. (6), as well as Elber and Kujawski models, Eqs. (2) and (4), is drawn for 2524-T3 aluminum alloy data.

2. The enhanced exponential model

Let β in Eq. (7) be a linear function of $\log R$, i.e., $\beta = \beta_0 + \beta_1 \log R$. Then Eq. (7) is re-written as Eq. (8), which

is linearized by defining the Y parameter presented in Eq. (9):

$$\frac{da}{dN} = \exp(\alpha) \exp\left(\frac{\beta_0 + \beta_1 \log R}{\Delta K}\right) \quad (8)$$

$$Y = \ln \frac{da}{dN} \Delta K = \alpha \Delta K + \beta_0 + \beta_1 \log R \quad (9)$$

where α , β_0 and β_1 are the fitting parameters to be determined and form a single group of constants, whatever the adopted R -ratio, i.e., they are in fact material constants. These are to be calculated by the least square method through the minimization of the total logarithmic error of crack growth prediction for all available experimental points from a group of FCG tests under different R -ratios.

The logarithmic square error is calculated as follows: Let r be the number of loading regimes and $p(j)$ the number of experimental points of curve “ j ”, $j = 1, \dots, r$. Thus the logarithmic error for point “ i ” of experimental curve “ j ” is:

$$E_{ij} = \ln \left(\frac{da}{dN} \right)_{ij} \Delta K_{ij} - \alpha \Delta K_{ij} - \beta_0 - \beta_1 \log R_j \quad (10)$$

The functional of total square error is given by Eq. (11):

$$E_T = \sum_{j=1}^r \sum_{i=1}^{p(j)} (E_{ij})^2 \quad (11)$$

The necessary minimum error conditions are determined by the system of Euler's equations, seen below. For the considered case, all 3 equations of system (12) are linear with respect to α , β_0 and β_1 ; therefore, the calculation of material constants is straightforward:

$$\begin{cases} \frac{\partial E_T(\alpha, \beta_0, \beta_1)}{\partial \alpha} = 0 \\ \frac{\partial E_T(\alpha, \beta_0, \beta_1)}{\partial \beta_0} = 0 \\ \frac{\partial E_T(\alpha, \beta_0, \beta_1)}{\partial \beta_1} = 0 \end{cases} \quad (12)$$

3. Experimental details

Fatigue crack growth data were collected from the high strength 2524-T3 aluminum alloy, commonly used in aircraft engineering applications. The material was received as plates with 6.35 mm in thickness and its basic mechanical properties, determined from tensile tests, are given in Table 1. Compact tension specimens, cut in the LT orientation, were adopted for this work. The FCG tests were conducted at room temperature in laboratory air using a MTS servo-hydraulic machine and were performed with constant load amplitude under force control. The test frequency was kept constant at 10 Hz and the loading waveform was sinusoidal. The following load ratios (min/max) were adopted for the tests: $R = 0.05, 0.1, 0.15, 0.30, 0.50$ and 0.60 . The compliance method of crack length

Table 1
Material properties.

Material specification	Yield stress (MPa)	UTS (MPa)	Elongation (%)
Al 2524-T3	340	450	21

monitoring was used during the tests and the five point incremental polynomial technique was employed for computing the crack growth rate. All of the experimental and numerical procedures were in conformity with the standard practice for Measurement of Fatigue Crack Growth Rates (ASTM E647-08e1). Crack closure measurements were performed in order to allow ΔK_{eff} calculations to be used in FCG modeling according to Elber's approach. The linear-quadratic spline method in which the "load versus COD" plots are modeled using two-section least square fit curves, was employed in closure calculations. The resulting FCG data were employed in the models development and comparison.

4. Results and discussion

In Fig. 2, the measured Region II crack growth rates, da/dN , from the six performed experiments are plotted against the corresponding nominal ΔK values in log–log scale. As expected, increasing the R ratio increases da/dN for a given ΔK . Moreover, a tendency of the experimental curves to be closer to each other as R increases can be inferred from the experimental data. These data are to be modeled according to Elber's, Kujawski's and UA potential equations taken from literature, as well as the new exponential model introduced in the present paper.

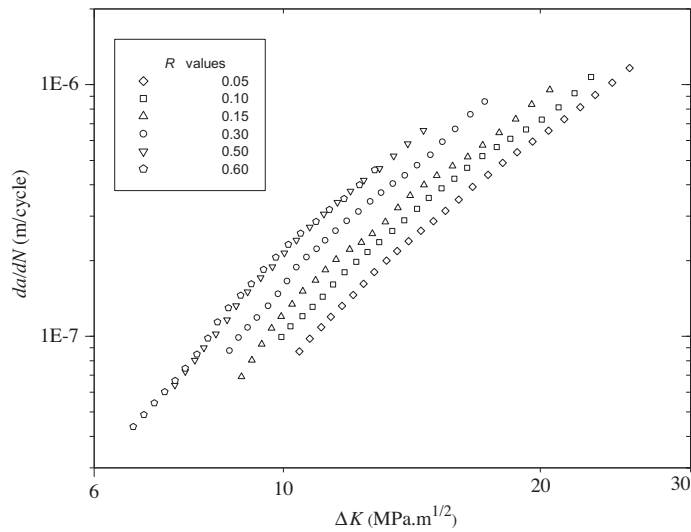


Fig. 2. Region II fatigue crack growth data of 2524-T3 aluminum alloy as a function of nominal ΔK for six distinct R -ratios.

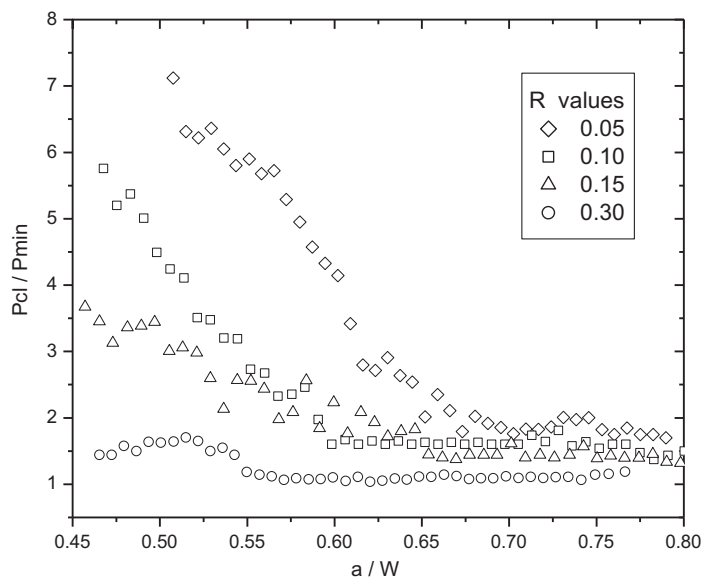


Fig. 3. Normalized closure load variation with crack size for 2524-T3 aluminum alloy.

4.1. Elber's model

From the closure measurements, the values of ΔK_{eff} were obtained according to Elber's approach. Significant closure was observed and measured for the tests performed at R -ratios of 0.05, 0.1 and 0.15; less pronounced closure at $R = 0.3$ and virtually no closure occurred at $R = 0.5$ and $R = 0.6$. Fig. 3 shows a plot of closure load results corresponding to the R -ratios for which significant closure was observed. The data are plotted in terms of the normalized closure load (P_{cl}/P_{min}), where P_{min} is the minimum load of the cycle, against the normalized crack length (a/W), where W is the specimen width. An important aspect verified in

Fig. 3 is that, for a given R , P_{cl} decreases as the crack length increases, and even approaches P_{min} at the end of stable crack growth regime. This means that closure description exclusively in terms of load ratio is not possible, making it difficult to predict crack closure and ΔK_{eff} for an untested R . The results FCG rate versus ΔK_{eff} are plotted in Fig. 4. By comparing with the results shown in Fig. 2, it is easily observed that the six experimental data sets become closer to each other when ΔK_{eff} is considered, except for the test at $R = 0.05$, which is dislocated in the graph. The representation of all tests by a single curve, as expected by the crack closure theory, results in $C = 9.16E-10$ and $n = 2.33$. The linear fitting coefficient of correlation R^2 is 0.959. The

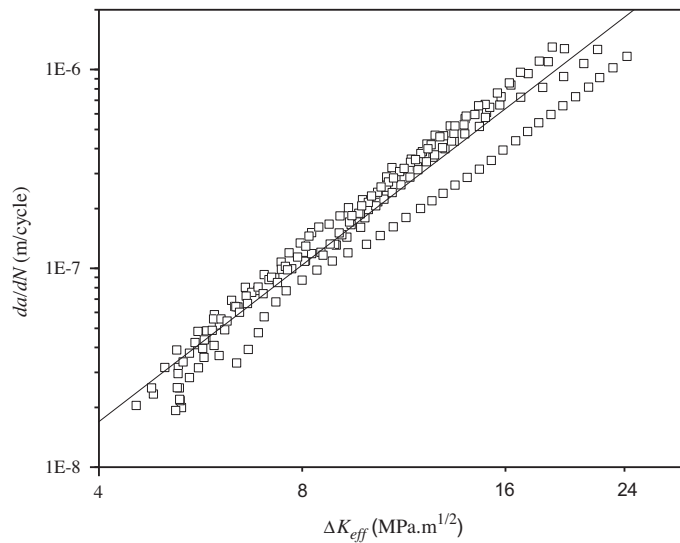


Fig. 4. Fatigue crack growth data of 2524-T3 aluminum alloy as a function of ΔK_{eff} and fitted to Elber's model.

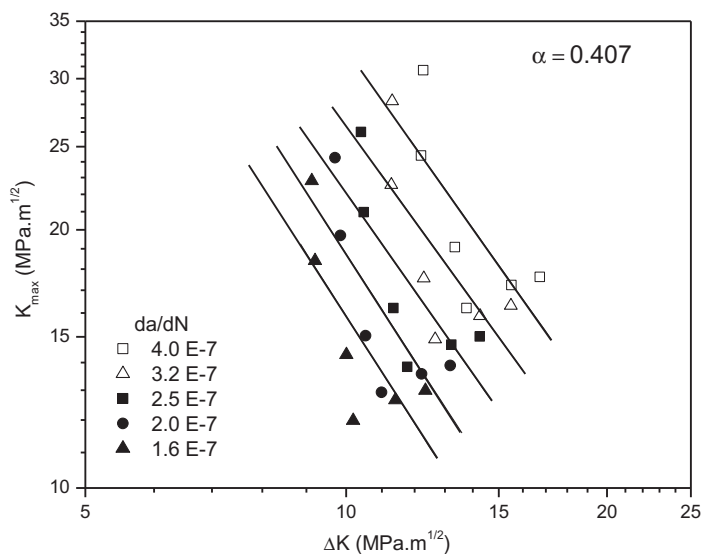


Fig. 5. ΔK versus K_{max} plots of 2524-T3 aluminum alloy used for determination of Kujawski's α -constant.

anomalous results at $R = 0.05$ and inevitable general noise in closure calculations contributed to this relatively low R^2 statistics.

4.2. Kujawski's model

FCG modeling with Eq. (4) is preceded by the determination of constant " α ". To do so, the experimental data were tri-dimensionally treated by using the computer program Catia™. In this environment the data representing ΔK , K_{max} and da/dN were manipulated respectively in the axes x , y and z . Curves representing the various loading conditions were numerically adjusted to the experimental points. By using arbitrarily chosen da/dN values, represented by planes parallel to xy plane, the ΔK and K_{max} values for a

given da/dN were determined from the intersections between these planes and the FCG curves. The obtained results, as well as the linear fittings from which individual α values were calculated, are shown in Fig. 5. An average $\alpha = 0.407$ was determined as the arithmetic mean of these values. The driving force parameter ΔK^* was then calculated for each experimental point and the resulting data set was fitted to Kujawski's model as shown in Fig. 6, resulting in $C = 6.57E-11$ and $n = 3.08$. The coefficient of correlation R^2 was 0.972.

4.3. "Unified" model

The experimental points corresponding to the six adopted loading ratios were simultaneously fitted to a

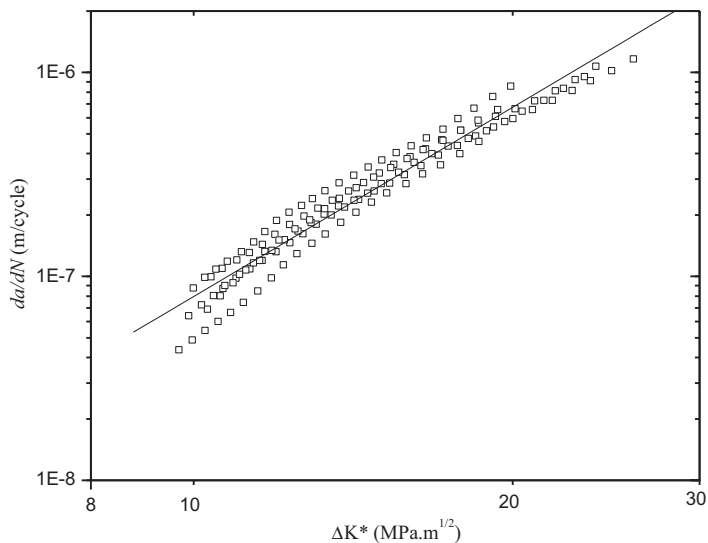


Fig. 6. Fatigue crack growth data of 2524-T3 aluminum alloy as a function of ΔK^* and fitted to Kujawski's model.

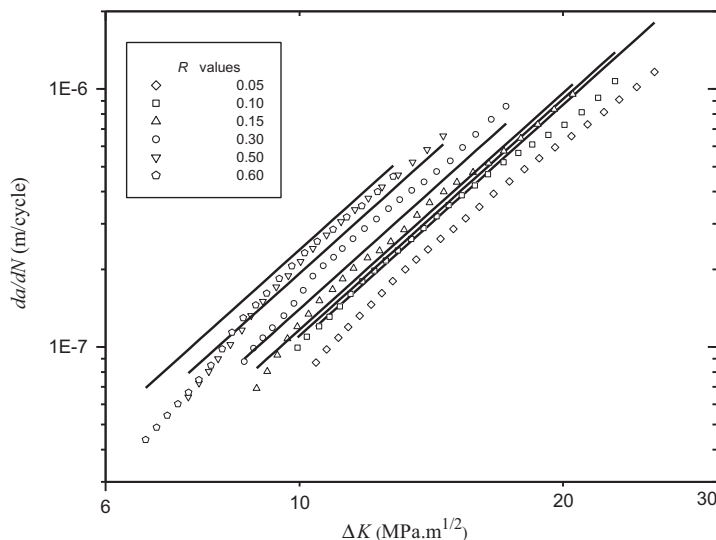


Fig. 7. Fatigue crack growth data of 2524-T3 aluminum alloy as a function of nominal ΔK and fitted to "unified" model.

two-parameter model in terms of ΔK and K_{max} , as seen in Eq. (6), by minimization of the logarithmic square error using an algorithm similar to that described in Eqs. (10)–(12). Thus, all of the experimental curves are to be described with a single group of fitting constants, for which the encountered values were: $C = 9.01E-11$, $\alpha = 2.10$ and $\beta = 0.946$. This “unified” model provides a set of parallel lines, which are shown in Fig. 7 superimposed to the experimental points in da/dN – ΔK plots. It is clear from Fig. 7 that the model tendency is opposite to “real” behavior as for the description of the R -effect, i.e., the curves become closer to each other as R decreases. This behavior, inherent to the adopted equation, limits the ability of the “unified” model in precisely describing the experimental curves.

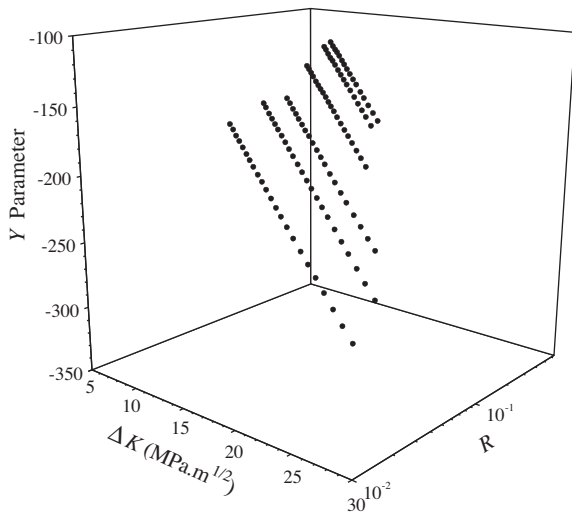


Fig. 8. 3D representation of fatigue crack growth data of 2524-T3 aluminum alloy.

4.4. Exponential model

For each experimental point, the Y parameter was determined according to Eq. (9) and plotted against ΔK and R in a 3-D graph, see Fig. 8. The points clearly form a plane, whose coefficients α , β_0 and β_1 were determined by solving the linear system of Eq. (12), resulting in: $\alpha = -11.96$, $\beta_0 = -30.88$ and $\beta_1 = 11.50$. The FCG rates were then calculated from Eq. (8) and plotted in Fig. 9. This figure allows observing that, besides adequately describing the R -effect, the exponential model also accounts for the slight deviations from linearity shown by the experimental points.

4.5. Model comparison

The efficacy of the tested models can be evaluated through the normalized sum of residuals corresponding to the set of experimental points of each curve and calculated according Eq. (13). In Table 2 these sums (multiplied by 10^2) are given for the Elber, Kujawski, “unified” and exponential models. From these results, the superior performance of the exponential model is evident. The conventional Elber’s model, that utilizes disputable crack closure data, presented the poorest correlation of the four tested models. The calculated residuals are also a numerical evidence that Region II fatigue cracks in Al 2524-T3 deviate

Table 2
Normalized sum of residuals for the tested models (10^2).

R	Elber	Kujawski	“Unified”	Exponential
0.05	28.0	1.7	11.9	0.23
0.10	2.5	1.4	2.1	0.02
0.15	2.9	0.9	0.7	0.24
0.30	1.3	4.9	1.8	0.18
0.50	2.5	1.2	1.2	0.13
0.60	2.2	13.2	9.6	0.25

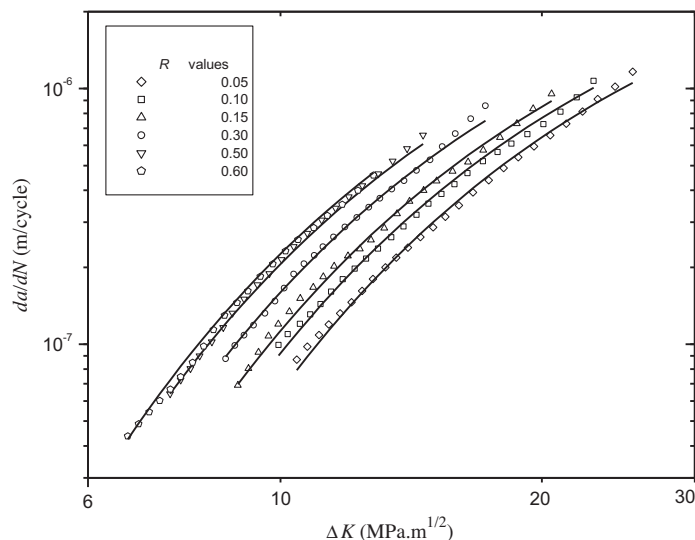


Fig. 9. Fatigue crack growth data of 2524-T3 aluminum alloy as a function of nominal ΔK and fitted to the enhanced exponential model.

from linearity are more precisely described by an exponential equation.

$$\text{Residue}(j) = \sum_{i=1}^{p(j)} \sqrt{\left(\frac{da/dN_{i,exp} - da/dN_{i,calc}}{da/dN_{i,exp}}\right)^2} / p(j) \quad (13)$$

5. Conclusion

In this work, an enhanced two-parameter exponential equation of FCG was introduced in order to describe sub-critical crack growth behavior of Al 2524-T3 alloy. By defining a so-called Y parameter, this new model preconizes the existence of a FCG plane of crack propagation in 3D plots against ΔK and R . It was demonstrated that besides adequately correlating the R -ratio effects, the exponential model also accounts for the slight deviations from linearity shown by the experimental curves. A comparison was made between the exponential model and other models aimed at describing FCG for a range of stress ratios: Elber, Kujawski and a “unified” model. By determining the normalized sum of residuals corresponding to the set of experimental points at each of six load ratios, it was verified that the exponential model, by its characteristics, presented a better performance when confronted to the other tested models.

References

- Adib, A.M.L., Baptista, C.A.R.P., 2007. An exponential equation of fatigue crack growth in titanium. *Mater. Sci. Eng. A*, USA 452–453, 321–325.
- Alizadeh et al., 2007. A comparison of two and three-dimensional analyses of fatigue crack closure. *Int. J. Fatigue* 29, 222–231.
- Baptista, C.A.R.P., Torres, M.A.S., Pastoukhov, V.A., Adib, A.M.L., 2006. Development and evaluation of two parameter models of fatigue crack growth. In: 9th International Fatigue Congress, Atlanta, USA, 10p (cd-rom).
- Broek, D., Shijve, J., 1963. The influence of the mean stress on the propagation of fatigue cracks in aluminum alloy sheets. Report NLR M 2111, National Aerospace Laboratory NLR, Amsterdam.
- Dowling, N.E., 1999. *Mechanical Behavior of Materials*. Prentice Hall, New Jersey.
- Elber, W., 1971. The significance of fatigue crack closure. In: *Damage Tolerance in Aircraft Structure*. ASTM STP 486, Philadelphia, p. 230–247.
- Forman, R.G., Kearney, V.E., Engler, R.M., 1967. Numerical analysis of crack propagation in cyclic loaded structures. *J. Basic Eng. Trans., ASME*, 459–464.
- Ishii, H., Choi, S.J., Tohgo, K., 1999. In: *International Conference on Mechanical Behavior of Materials, ICM8*, Victoria, Canada, Proceedings, v.1.2, pp. 73–78.
- Ismonov, S., Daniewicz, S.R., 2010. Simulation and comparison of several crack closure assessment methodologies. *Int. J. Fatigue* 32, 428–433.
- Jones, R., Molent, L., Pitt, S., 2008. Similitude and the Paris crack growth law. *Int. J. Fatigue* 30, 1873–1880.
- Kohout, J., 1999. A new function describing fatigue crack growth curves. *Int. J. Fatigue* 21, 813–821.
- Kujawski, D., 2001. A new $(\Delta K^* K_{max})^{0.5}$ driving force parameter for crack growth in aluminum alloys. *Int. J. Fatigue* 23, 733–740.
- Kujawski, D., Dinda, S., 2004. Correlation and prediction of fatigue crack growth for different R -ratios using K_{max} and ΔK^* parameters. *Eng. Fract. Mech.* 71, 1779–1790.
- Lee, Y.L., Pan, J., Hathaway, R., Barkey, M., 2005. *Fatigue Testing and Analysis: Theory and Practice*. Amsterdam: Elsevier, Butterworth Heinemann.
- Louat, N., Sadananda, K., Duesbery, M., Vasudevan, A.K., 1993. A theoretical evaluation of crack closure. *Metall. Trans. A* 24A, 2225–2232.
- Macha, D.E., Corby, D.M., Jones, J.W., 1979. On the variation of fatigue crack opening load with measurement location. *Proc. Soc. Exp. Stress Anal.* 36, 207–213.
- Maymon, G., 2005. A “unified” and a $(\Delta K^* K_{max})^{1/2}$ crack growth models for aluminum 2024-T351. *Int. J. Fatigue* 27, 629–638.
- McClung, R.C., 1991. The influence of applied stress, crack length and stress intensity factor on crack closure. *Metall. Trans. A* 22A, 1559–1571.
- McEvily, A.J., Ritchie, R.O., 1998. Crack closure and the fatigue crack propagation threshold as a function of load ratio. *Fatigue Fract. Eng. Mater. Struct.* 21, 847–855.
- Molent, L., Barter, S.A., 2007. A comparison of crack growth behavior in several full-scale airframe fatigue tests. *Int. J. Fatigue* 29, 1090–1099.
- Newman, J.C., Elber, W. (Eds.), 1988. *Mechanics of fatigue crack closure*. In: *Proceedings of the International Symposium on Fatigue Crack Closure*. ASTM STP 982, Philadelphia.
- Noroozi, A.H., Glinka, G., Lambert, S., 2007. A study of the stress ratio effects on fatigue crack growth rate using the unified two-parameter fatigue crack growth driving force. *Int. J. Fatigue* 29, 1616–1633.
- Paris, P., Erdogan, F., 1963. A critical analysis of crack propagation laws. *J. Basic Eng. Trans., ASME*, 528–534.
- Philips, E.P., 1989. Results of the round robin on opening load measurement conducted by ASTM Task Group E24.04.04 on crack closure measurements and analysis. NASA TM-101601.
- Ritchie, R.O., Suresh, S., 1982. Some considerations on fatigue crack closure at near-threshold stress intensities due to fracture surface morphology. *Metall. Trans. A* 13A, 937–940.
- Sadananda, K., Vasudevan, A.K., 1999. Unified Approach fatigue crack growth. In: *ICM8, 1999, International Conference on Mechanical Behavior of Materials*, Victoria, Canada, Proceedings, V.1.6, pp. 283–288.
- Sadananda, K., Vasudevan, A.K., 2003a. Multiple mechanisms controlling fatigue crack growth. *Fatigue Fract. Eng. Struct.* 26, 835–845.
- Sadananda, K., Vasudevan, A.K., 2003b. Fatigue crack growth mechanisms in steels. *Int. J. Fatigue* 25, 899–914.
- Sadananda, K., Vasudevan, A.K., 2004. Crack tip driving forces and crack growth representation under fatigue. *Int. J. Fatigue* 26, 39–47.
- Shin, C.S., Smith, R.A., 1985. Fatigue crack growth from sharp notches. *Int. J. Fatigue* 7, 87–93.
- Skelton, R.P., Haigh, J.R., 1978. Fatigue crack growth rates and thresholds in steels under oxidising conditions. *Mater. Sci. Eng.* 36, 17–25.
- Stephens, R.I., Fatemi, A., Stephens, R.R., Fuchs, H.O., 2001. *Metal Fatigue in Engineering*, second ed. John Wiley & Sons, New York.
- Suresh, S., 1998. *Fatigue of Materials*, second ed. Cambridge University Press, Cambridge.
- Swain, M.H., Everett, R.A., Newman, Jr, J.C., Philips, E.P., 1990. In: *Edwards, P.R., Newman, Jr., J.C. (Eds.), Short Crack Growth Behavior in Various Aircraft Materials*, AGARD, R-767, pp. 7.1–7.30.
- Vasudevan, A.K., Sadananda, K., 1996. Fatigue crack growth in advanced materials. In: *Lütjering, G., Nowack, H. (Eds.), Fatigue'96, Proceedings of the 6th International Conference on Fatigue*, vol. 1. Pergamon Press, Oxford, pp. 473–478.
- Walker, K., 1970. The effect of stress ratio during crack propagation and fatigue for 2024-T3 and 7075-T6 aluminium. In: *Effects of Environment and Complex Loading History on Fatigue Life*. ASTM STP 462, Philadelphia, p. 1–14.
- Xiaoping, H., Torgeir, M., 2007. Improved modeling of the effect of R -ratio on crack growth rate. *Int. J. Fatigue* 29, 591–602.
- Zhang, J., He, X.D., Du, S.Y., 2005. Analyses of the fatigue crack propagation process and stress ratio effects using the two parameter method. *Int. J. Fatigue* 27, 1314–1318.